MOLECULAR PHARMACOLOGY, 20:89-97



# Internal Flexibility of Inhibitors Bound to *Electrophorus electricus* Acetylcholinesterase

## Proton Nuclear Magnetic Resonance Spectroscopy

ALAN G. MARSHALL[1] AND JUNKO M. CARRUTHERS

*Departments of Chemistry and Biochemistry, Ohio State University, Columbus, Ohio 43210*

Received July 28, 1980; Accepted February 9, 1981

SUMMARY

MARSHALL, A. G., AND J. M. CARRUTHERS. Internal flexibility of inhibitors bound to *Electrophorus electricus* acetylcholinesterase: proton nuclear magnetic resonance spectroscopy. *Mol. Pharmacol.* **20**:89-97 (1981).

Flexibility of each of five inhibitors of acetylcholinesterase (AchE) has been determined from proton NMR line width of the inhibitor methyl peak on binding to 11.8 S AchE and to 11.8 S AchE previously carbamylated or sulfonylated at the active-site serine residue. When bound to unmodified AchE, all studied inhibitors show high rotational lability. For carbamylated or sulfonylated enzyme, inhibitor flexibility decreases as inhibitor size increases. The results suggest that these inhibitors (trimethylammonium, phenyltrimethylammonium, *cis*-2,6-dimethylspiro(piperidine-1,1-pyrrolidinium), atropine, and eserine) bind in a spatious anionic pocket near the active-site serine residue.

### INTRODUCTION

Proton NMR spectroscopic line width for a small molecule binding reversibly and rapidly to a macromolecule in solution can provide a direct measure of the flexibility (1, 2) of an inhibitor or substrate at its binding site on the enzyme. Comparison of the rotational freedom for several bound inhibitors of different size and shape can then give direct information about the size and shape of the binding site(s).

Despite the central importance of AchE[2] (EC 3.1.1.7) as the enzyme that hydrolyzes the neurotransmitter acetylcholine at cholinergic synapses, there have been no NMR studies of substrate or inhibitor binding to highly purified AchE. The relatively few attempts to use NMR to study substrate (3-6) and inhibitor (7-10) binding to AchE were based on experiments at a single temperature, using AchE whose specific activity was at best about one-third that of the affinity-purified enzyme, with continuous wave-scanning techniques at a single (relatively low) magnetic field. The results were inconclusive and inconsistent. For example, four independent determinations by Kato *et al.* (7-10) of the bound line width for the atropine *N*-methyl protons gave values of 6750 Hz (8), 2200 Hz (7), 1780 Hz (9), and 858-984 Hz (5, 10). All four values are larger than is theoretically possible (see below) for unaggregated enzyme.

The principal problem in previous work has been the difficulty of obtaining AchE in high yield, at high specific activity, and in stable form. Recent affinity chromatography techniques (11-14) have made possible the isolation of milligram quantities of AchE in a form (11.8 S) that is relatively stable toward autolysis, with a specific activity that is as high as for the "tailed" 18 S enzyme. The 11.8 S form is a globular tetramer consisting of four identical subunits (15, 16); the active unit may thus be considered to be an 80,000 mol wt component of a 320,000 mol wt macromolecule.

In this paper, we report a reinvestigation of the interaction of eserine and atropine with 11 S AchE, with completely different results. The present experiments involve FT-NMR to permit signal averaging to improve the signal-to-noise ratio (and thus the reliability) of the results, at two magnetic fields, at two temperatures, using affinity-purified AchE of high specific activity. In addition, the interaction of three inhibitors with methanesulfonylated AchE is reported; the methanesulfonyl moiety is covalently bound to the esteratic serine residue and should thus offer steric hindrance to any inhibitor bound to a nearby site. The present experiments can be interpreted by using a single format, and offer direct evidence

This work was supported by grants (to A.G.M.) from the National Sciences and Engineering Research Council of Canada (A-6178), the University of British Columbia (21-9879), Ohio State University, and the Alfred P. Sloan Foundation.

[1] Alfred P. Sloan Research fellow, 1976-1980.

[2] The abbreviations used are: AchE, acetylcholinesterase (acetylcholine hydrolase); FT-NMR, Fourier transform NMR; TSP, sodium 3-trimethylsilylpropionate-2,2,3,3-$d_4$.

0026-895X/81/010089-09$02.00/0

for the spatial proximity of the "anionic" and "esteratic" sites on the enzyme (see Discussion).

## THEORY

In the present experiments, the observed proton NMR signal arises from methyl groups of inhibitor molecules that may be either free in solution or bound to AchE enzyme. The observed proton NMR line width depends upon the exchange rate constants for binding and dissociation of the enzyme/inhibitor complex, the difference in chemical shift (if any) between free and bound inhibitor, and the degree of rotational flexibility at the free and bound sites. In order to extract the flexibility information, it is necessary to summarize the effects of chemical exchange upon NMR line width.

The simplest useful model for two-site exchange, in the absence of scalar ("J") spin-spin coupling, is based on the original modification by McConnell (17) of the Bloch equations describing the time dependence of the nuclear magnetization. Since free inhibitor (Site $A$) concentration is much larger than bound inhibitor (Site $B$) concentration in all of the present experiments, the simplified explicit result of Swift and Connick (18) gives the following expression for the steady-state $v$-mode (absorption mode; 90° out-of-phase response) signal, $v$

$$v = \frac{\omega M_{0_A}\left[\frac{1}{T_{2_A}} + P_{AB}\left\{\frac{\left(\frac{1}{T_{2B}}\right)^2 + \frac{P_{BA}}{T_{2B}} + (\Delta\omega_B)^2}{\left(\frac{1}{T_{2B}} + P_{BA}\right)^2 + (\Delta\omega_B)^2}\right\}\right]}{\left[\frac{1}{T_{2A}} + P_{AB}\left\{\frac{\left(\frac{1}{T_{2B}}\right)^2 + \frac{P_{BA}}{T_{2B}} + (\Delta\omega_B)^2}{\left(\frac{1}{T_{2B}} + P_{BA}\right)^2 + (\Delta\omega_B)^2}\right\}\right]^2 + \left[\Delta\omega_A + \frac{P_{AB}P_{BA}\Delta\omega_B}{\left(\frac{1}{T_{2B}} + P_{BA}\right)^2 + (\Delta\omega_B)^2}\right]^2} \quad (1)$$

in which $T_{2A}$ and $T_{2B}$ are the transverse relaxation times at Sites $A$ and $B$, $P_{AB}$ and $P_{BA}$ are the reciprocal lifetimes for association and dissociation

$$\Delta\omega_A = \omega_{0_A} - \omega \quad (2a)$$

$$\Delta\omega_B = \omega_{0_B} - \omega \quad (2b)$$

in which $\omega_{0_A}$ and $\omega_{0_B}$ are the Larmor frequencies at sites $A$ and $B$, $\omega$ is the observing frequency, and $M_{0_A}$ is the equilibrium $z$-magnetization at Site $A$.

As noted in ref. 18, the maximal value of $v$ occurs when the second term in the denominator of Eq. 1 is 0 leaving a Lorentzian line shape whose full width at half-maximal height is given by

$$\frac{1}{T_2} = \frac{1}{T_{2A}} + P_{AB}\left[\frac{\left(\frac{1}{T_{2B}}\right)^2 + \frac{P_{BA}}{T_{2B}} + (\Delta\omega)^2}{\left(\frac{1}{T_{2B}} + P_{BA}\right)^2 + (\Delta\omega)^2}\right]; \Delta\omega = \omega_B - \omega_A \quad (3)$$

It is convenient to consider three limiting exchange rate cases, summarized in Table 1 as "slow," "intermediate," and "fast." In the slow limit, $\omega_A = \omega$, since the only visible peak is centered at the Larmor frequency of free $A$ molecules. The $\omega_A$ value is also equal to $\omega$ in the fast-exchange limit, because the frequency of the exchange-averaged peak is very close to that of free $A$, owing to the $[A] \gg [B]$ condition. In the slow limit, line broadening is determined by the exchange lifetime; in the fast limit, broadening is determined by the "bound" line width, $\Delta\nu_B = (1/\pi T_{2B})$; in the intermediate limit, broadening is affected both by the exchange lifetime and the change in chemical shift on binding. The flexibility information contained in $T_{2B}$ is thus accessible only in the fast-exchange limit, and it thus becomes necessary (see Results and Discussion) to establish the exchange limit before interpreting experimental line broadening data.

In the fast-exchange limit

$$\frac{1}{T_2} - \frac{1}{T_{2A}} = f_B\frac{1}{T_{2B}} \quad (4)$$

TABLE 1

*Limiting expressions for transverse nuclear magnetic relaxation time for two-site exchange, $A \rightleftharpoons B$, for $[A] \gg [B]$ (see Eq. 3 ff)*

| Limit | Range of validity | $\frac{1}{T_2} - \frac{1}{T_{2A}}$ | Available information[a] |
|---|---|---|---|
| Slow | $P_{BA}^2, \left(\frac{1}{T_{2B}}\right)^2 \ll (\Delta\omega_B)^2$ | $f_B P_{BA}$ | $P_{BA}$; $K_D$ |
| or | $(\Delta\omega_B)^2, P_{BA}^2 \ll \left(\frac{1}{T_{2B}}\right)^2$ | | |
| Intermediate | $\frac{P_{BA}}{T_{2B}} \ll (\Delta\omega_B)^2 \ll P_{BA}^2$ | $\frac{f_B(\Delta\omega_B)^2}{P_{BA}}$ | $\frac{(\Delta\omega_B)^2}{P_{BA}}$; $K_D$ |
| Fast | $(\Delta\omega_B)^2, \left(\frac{1}{T_{2B}}\right)^2 \ll \frac{P_{BA}}{T_{2B}}$ | $f_B\left(\frac{1}{T_{2B}}\right)$ | $\frac{1}{T_{2B}}$; $K_D$ |

[a] $f_B = \frac{P_{AB}}{P_{AB} + P_{BA}} \cong \frac{P_{AB}}{P_{BA}}$

= fraction of inhibitor molecules bound to enzyme.

$K_D = \frac{[E][I]}{[EI]}$

= dissociation constant for enzyme/inhibitor complex.

in which

$$f_B = \frac{P_{AB}}{P_{AB} + P_{BA}} = \frac{[EI]}{[I] + [EI]} \quad (5)$$

is the fraction of inhibitor molecules bound to enzyme. Next, from the equilibrium dissociation constant for the enzyme/inhibitor ($EI$) complex

$$K_D = \frac{[E][I]}{[EI]} = \frac{([E]_0 - [EI])[I]_0}{[EI]} \quad (6)$$

in which $[E]_0$ and $[I]_0$ are the total concentrations of enzyme (bound or free) and inhibitor (bound or free), and $[I] = [I]_0$ because $[I]_0 \gg [E]_0$, we may solve Eq. 6 for $[EI]$ and substitute for $[EI]$ in $f_B$ to obtain

$$\frac{1}{T_2} - \frac{1}{T_{2A}} = \frac{[E]_0}{[I]_0 + K_D}\left(\frac{1}{T_{2B}}\right) \quad (7)$$

Alternatively, we may rearrange Eq. 7 by solving for $[I]_0$ to give

$$I_0 = \frac{[E]_0}{\frac{1}{T_2} - \frac{1}{T_{2A}}}\left(\frac{1}{T_{2B}}\right) - K_D \quad (8)$$

The transverse relaxation rate, $(1/T_{2B})$, for bound inhibitor may thus be obtained from either: (a) the slope of a plot of $[(1/T_2) - (1/T_{2A})]$ versus $[E]_0/([I]_0 + K_D)$, or (b) the slope of a plot of $[I]_0$ versus $[E]_0/[(1/T_2) - (1/T_{2A})]$. It is necessary to know $K_D$ in advance in order to use Method (a), but not for Method (b): Both methods will be used to analyze the present results.

Finally, the effect of internal flexibility upon the transverse relaxation rate, $(1/T_{2B}) = \pi\Delta\nu_B$, of the bound inhibitor, in which $\Delta\nu_B$ is the line width at half-maximal height for the bound inhibitor, has been treated by Werbelow and Marshall (19, 20) for a methyl group rigidly bound to a spherical macromolecular frame, from which the expected dependence of $(1/T_{2B})$ upon macromolecular rotational correlation time, $\tau_{rot}$, may be calculated. The value for $\tau_{rot}$ may in turn be estimated from the Stokes-Einstein equation

$$\tau_{rot} = \frac{4\pi\eta R^3}{3kT} \quad (9)$$

in which $\eta$ is viscosity in centipoise when $R$ is macromolecular radius in centimeters, $T$ is temperature in Kelvin units, and $k$ is Boltzmann's constant = $1.38 \times 10^{-16}$ erg $K^{-1}$. The molecular radius may be estimated from ref. 21

$$R = \left[\frac{3M}{4\pi N_0}(\bar{v}_{macro} + \delta\,\bar{v}_{solvent})\right]^{1/3} \quad (10)$$

in which $M$ is the macromolecular weight, $N_0$ is Avogadro's number, and $\bar{v}$ is partial specific volume for solute or solvent. For example, for 11 S AchE, assuming $M$ = 320,000, with $\bar{v}_{macro} = 0.72$ ml/g, spherical shape, and zero degree of hydration, $\delta$, we obtain a rotational correlation time of approximately, $\tau_{rot}$ = 92 nsec. From refs. 19 and 20, $(1/T_{2B})$ is then determined to be about 1260 sec$^{-1}$, to give a bound line width, $\Delta\nu_B$ = 400 Hz. For a more realistic degree of hydration of $\delta$ = 0.2 g of water per gram of protein, $\Delta\nu_B$ = 500 Hz.

## MATERIALS AND METHODS

*Enzyme isolation and purification.* Live electric eels (2 feet long) were killed by packing them in crushed ice for ½ hr. The following procedures (14) were followed in order to avoid autolysis. Homogenized tissue was centrifuged, rehomogenized, and centrifuged in 5% sucrose, then resuspended and centrifuged in high-salt buffer, and eluted from an *N*-methyl-acridinium-coupled Sepharose 2B affinity matrix with decamethonium. AchE activity was 9 mmoles of acetylthiocholine hydrolyzed per minute per milligram of protein, based on the published AchE extinction coefficient, $\epsilon^{1\%}_{280nm}$ = 18.0.

*Conversion of AchE to 11 S form.* The AchE solution was dialyzed against 100 volumes of trypsin buffer at 4° twice for 24 hr. One milligram of trypsin was added per 25 ml of AchE solution ($A_{280}$ = 0.7) and incubated at room temperature for 1 hr. The reaction was terminated by addition of soybean trypsin inhibitor at 2 mg/25 ml of AchE solution. (AchE activity was unchanged by this trypsin treatment.) This procedure gave AchE with nearly 100% conversion to the 11 S form without loss in activity.

Conversion to the 11 S form was monitored by using sucrose gradient isokinetic sedimentation. The exponential sucrose gradient (22) was prepared by pumping a 29.3% sucrose solution in chromatography buffer (20 mM sodium phosphate, 1 M NaCl, pH 7.0) into a 10% sucrose solution in the same buffer, which in turn was pumped at exactly the same speed (peristaltic pump) into gradient tubes (7.3-cm cellulose nitrate tubes for Beckman SW 41 swinging bucket rotor). At 4°, a thin layer of solution containing AchE (100 μl; 300–1000 activity units) and 100 μl of standards [β-galactosidase, 15.9 S (23); catalase, 11.3 S (11)] in 10% sucrose solution was applied to the top of the gradient tube and centrifuged at 40,000 rpm for 1,920 hr in a Beckman 2350 ultracentrifuge.

After centrifugation, fractions were removed by carefully lowering a capillary to the bottom of the tube and withdrawing 0.5-ml aliquots. AchE concentration was determined by its activity, catalase by its characteristic 405-nm absorption, and β-galactosidase by a specific activity assay. Figure 1 shows the sucrose gradient profiles before and after trypsin treatment. It is clear that the higher molecular weight forms of native AchE are converted almost completely to the globular, tetrameric, homogeneous 11 S form by the above trypsin treatment. The enzyme retained its integrity (based on sucrose gradient sedimentation profile) for 1 month in 4 M NaCl buffer (20 mM phosphate, pH 7.0).

*Concentration of AchE into $D_2O$ buffer.* Proton NMR experiments require relatively high protein concentration, preferably in $D_2O$ buffer to reduce the size of the $H_2O$ or HDO solvent signal. However, conventional freeze-drying (after passing AchE through Sephadex G-25 to remove decamethonium) denatured the enzyme.

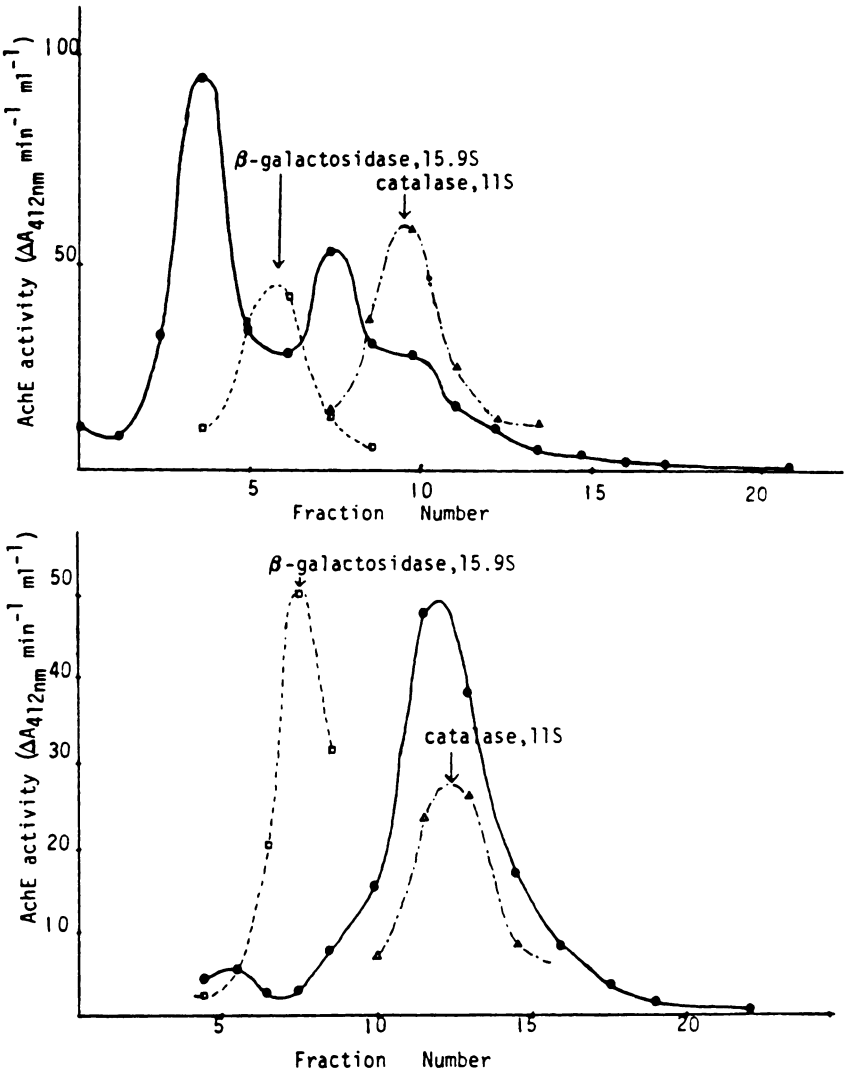


FIG. 1. *Isokinetic sucrose density gradient sedimentation profile of eel AchE, before (top) and after (bottom) treatment with trypsin*

Even under favorable conditions (sample frozen in 5% glycerol at liquid nitrogen temperature), only 35% of the original enzyme activity could be recovered (although all the protein was recovered).

A second method, based on the higher specific gravity of $D_2O$ compared with that of $H_2O$, involved layering a concentrated AchE sample (in tritiated $H_2O$) on top of $D_2O$ buffer in a centrifuge tube, then centrifuging for several hours. Tritium counting and AchE activity assay of the resultant tube aliquots showed that AchE could indeed be concentrated near the tube bottom (i.e., in $D_2O$), but it proved difficult in practice to stop the centrifuge exactly at the moment when enzyme was highly concentrated near the bottom but not yet pelletized. Attempts to slow the sedimentation near the tube bottom by change in density from added salts or sucrose failed.

The third (and successful) concentration method was to concentrate a 10-ml solution of AchE almost to nil volume, by applying 14–20 psi pressure to an Amicon Diaflo ultrafiltration cell equipped with a UM10 filter that had previously been equilibrated with chromatography buffer. The apparatus was then topped up with approximately 10 ml of $D_2O$ buffer (0.1 M NaCl, 20 mM sodium phosphate, pH meter reading 7.0), and the solution was again concentrated almost to nil volume. The process was repeated once more, and $D_2O$ buffer was added to give a final $A_{280}$ reading of about 3.5, corresponding to ~18 μM of 80,000 mol wt catalytic subunits of AchE, after correcting for the contributions from trypsin and trypsin inhibitors. This method recovered 65–75% of total enzyme, with no significant loss in activity.

In order to test for possible aggregation of AchE in low-salt media, even in a form (11 S) that does not contain a "tail," the relatively high-concentration NMR samples were tested for homogeneity by sucrose gradient centrifugation. A single, symmetrical sucrose gradient peak at 11 S was obtained even after storage at 30° for 12 hr or 17° for 24 hr, suggesting that aggregation of AchE is not significant under the NMR conditions of the present experiments.

*Preparation of eseroline.* Eseroline, Structure *6*, the hydrolysis product of eserine, was prepared by the method of Ellis (24). The product was recrystallized from a mixture of benzene and petroleum ether, and gave a melting point of 113–115°, with parent ion mass spectral peak at $m/e = 218$.

*Sulfonylation of AchE.* Ten grams of methanesulfonyl

chloride and 30 g of 70% aqueous KF solution were distilled and the fraction boiling at 124–125° was collected. Since the infrared spectrum showed the presence of a small amount of unreacted methanesulfonyl chloride, the organic layer was washed thoroughly with cold water to hydrolyze residual starting material. Redistillation gave pure methanesulfonyl fluoride, b.p. 125°, with parent ion mass spectral peak at 98 *m/e*.

A stock solution of 200 μl of $MeSO_2F$ in 5 ml of isopropanol (isopropanol does not decrease AchE activity at concentrations up to 2%) was added to a solution of 11 S AchE, followed by a second aliquot of $MeSO_2F$ after 2 hr, up to a 500-fold molar excess of $MeSO_2F$ over AchE, and the mixture was incubated at room temperature. After 6 hr, the AchE activity had decreased to 1/1000 of its original level, and the inhibited enzyme did not recover that lost activity for at least 4 days. The methanesulfonyl AchE was concentrated into $D_2O$ buffer as previously described, thereby removing excess $MeSO_2F$ and isopropanol at the same time.

*$^1$H NMR measurements.* Proton FT-NMR spectra were recorded either with a Varian XL-100 FT-NMR or Nicolet-Oxford 270 FT-NMR spectrometer. Three hundred microliters (XL-100) or 500 μl (270 MHz) of the 11 S AchE solution were mixed with a small volume (~35 μl) of $D_2O$ buffer containing the desired concentration of inhibitor and TSP, and injected into a 5-mm NMR tube. After temperature equilibration (30–45 min), as judged by shift of less than 0.1 Hz in 5 min for the TSP peak, the magnet homogeneity was adjusted to give a TSP line width of 0.8 Hz or less. position and peak width of the TSP signal were checked before and after each measurement to ensure magnetic field stability during signal acquisition; the spectrum was discarded if a TSP peak shift of more than 0.2 Hz or TSP broadening of more than 0.2 Hz was found.

Inhibitor concentration was increased by adding a known aliquot of concentrated stock solution to the same NMR tube sample, followed by temperature equilibration and homogeneity readjustment as above. In addition, the spectrum of each inhibitor in neat $D_2O$ buffer was recorded separately; no concentration dependence of free inhibitor line width was observed in this concentration range.

The amplitude of the residual HDO peak located near the signals of interest was reduced (approximately 20-fold) by use of a notch filter (25) in series with the usual low-pass filter (typically 100-Hz cutoff frequency). Typical 100-MHz (270 MHz in brackets) conditions were as follows: spectral width = 100–130 Hz (200 Hz), acquisition time = 5 sec (5.12 sec), pulse delay = 0 (393.22 msec), pulse width = 25 μsec (6.50 μsec), sensitivity enhancement = 3 sec (none), spin rate = 35–40 cps, temperature = 17–30° (17°), number of transients = 300–1000.

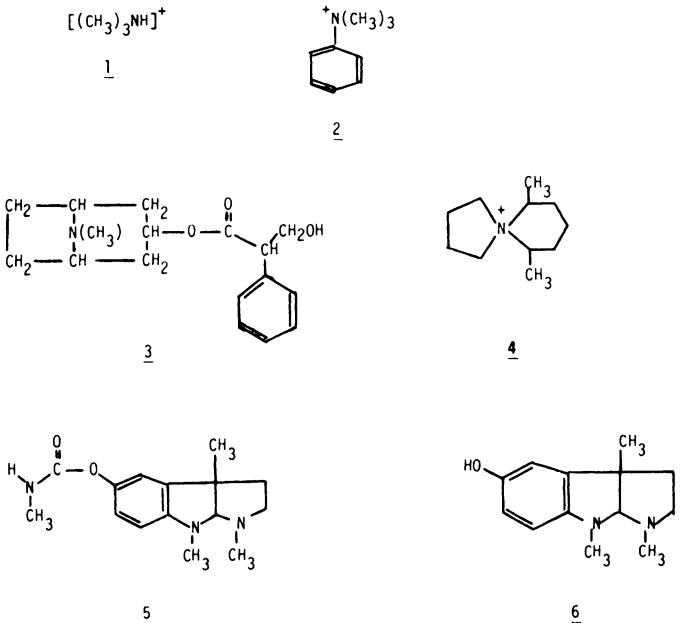


STRUCTURES 1-6

*1*, Trimethylammonium ion; *2*, phenyltrimethylammonium ion; *3*, atropine; *4*, *cis*-2,6-dimethylspiro(piperidine-1,1-pyrrolidinium) ion; *5*, eserine; *6*, eseroline.

## RESULTS

*Unmodified enzyme.* The $^1$H-FT-NMR spectrum of each of the inhibitors, Structures *1–5*, was recorded in the presence and absence of AchE. Figure 2 shows a typical result for atropine, Structure *3*. The line widths were corrected for change in viscosity on addition of protein by subtracting the line width of the (nonbinding) reference compound, TSP, from the line width of the inhibitor methyl group, as listed in Table 2 for Inhibitors *1–3*.

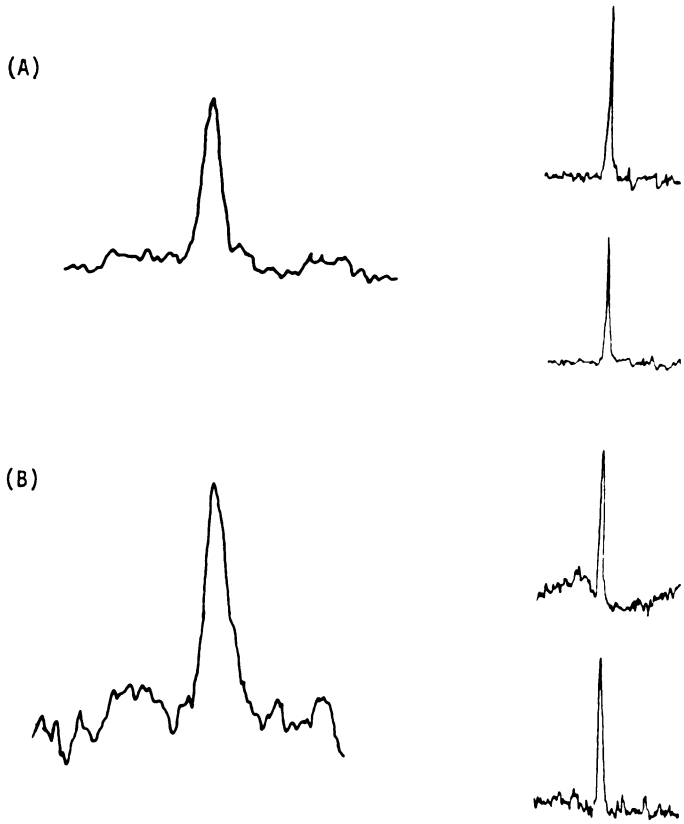


FIG. 2. *Methyl $^1$H-NMR spectrum of atropine without (A) and with (B) AchE*

The corresponding spectrum for the internal TSP reference peak, shown on the *right*, was recorded before (*top*) and after (*bottom*) the atropine peak at the *left*. The TSP abscissa has been reduced compared with that for atropine, and the line widths for the peaks are listed in Table 1.

TABLE 2

*Observed $^1H$ NMR line width changes for three inhibitors on binding to 11 S unmodified AchE*

| Inhibitor | Concentration | | Temperature | Observed line width, $\Delta\nu$ | | Net broadening, $\Delta\Delta\nu$,[b] due to binding of inhibitor to AchE |
|---|---|---|---|---|---|---|
| | Inhibitor | AchE[a] | | Inhibitor | TSP | |
| | *mM* | *μM* | | *Hz* | *Hz* | *Hz* |
| Atropine | 0.3 | — | 30° | 1.0 ± 0.1 | 0.5 ± 0.1 | 0.1 ± 0.14 |
| | 0.3 | 15 | 30 | 1.4 ± 0.1 | 0.8 ± 0.1 | |
| trimethylammonium chloride | 0.5 | — | 30 | 0.6 ± 0.1 | 0.5 ± 0.1 | 0.0 ± 0.2 |
| | 0.5 | 14.6 | 30 | 0.8 ± 0.1 | 0.7 ± 0.1 | |
| phenyltrimethylammonium chloride | 0.8 | — | 19 | 0.6 ± 0.1 | 0.6 ± 0.1 | 0.1 ± 0.14 |
| | 0.8 | 15 | 19 | 0.9 ± 0.1 | 0.8 ± 0.1 | |

[a] Concentration of 80,000 mol wt 11 S subunits.

[b] Computed as the difference between the increase in inhibitor line width and the increase in TSP line width on addition of AchE.

In marked contrast to previous observations (7–10), it is clear that the net line broadening for Inhibitors *1–3* is zero, within experimental error. Some line broadening was observed for the spiro compound, Structure *4*, but the broadening could not be quantified because the observed peak is in fact a multiplet whose over-all line width is not related in an easily determined way to the width of each component line.

*Carbamylated enzyme.* In previous $^1H$ NMR experiments (7–10), eserine (Structure *5*) was treated as a reversible inhibitor, binding to *unmodified* enzyme. However, eserine at these high concentrations is in fact an irreversible inhibitor of AchE, with $K_i = 3.3 \times 10^{-6}$ M and $k_2 = 10.8\ min^{-1}$ (26). At the present experimental concentrations of eserine and AchE, the time required for irreversible carbamylation of 99% of the available AchE is approximately 1 min; even less time would be required at the higher eserine concentrations in previous experiments (7–10). The hydrolysis product of this reaction is called eseroline, Structure *6*. Any observed change in eserine NMR line width in the presence of AchE is thus due to binding of eserine to *carbamylated* AchE.

The broadening of the eserine *C*-methyl resonance on binding to carbamylated AchE was large enough to measure, and the bound line width was extracted by use of the graphs (Figs. 3A and B) corresponding to Eqs. 7 and 8 (see Discussion).

*Sulfonylated enzyme.* Inhibitors *1–3* were exposed to methanesulfonyl AchE. Although no line broadening of the $^1H$-NMR methyl peak was observed for Inhibitor *1*, the measurable broadening for Inhibitors *2* and *3* made possible the graphical determination of bound line width for those inhibitors shown in Figs. 4 and 5.

The bound line widths for the various inhibitor/enzyme combinations described above are collected in Table 3, and are now analyzed.

## DISCUSSION

*Unmodified enzyme.* Since the data in Table 2 correspond to inhibitor concentrations that are lower than those used by Kato *et al.* (7–10), the observed line broadening should have been even larger than that observed by Kato *et al.* However, the observed line broadening was (within experimental error) *zero* for Inhibitors *1–3*. One explanation is that the AchE was denatured or

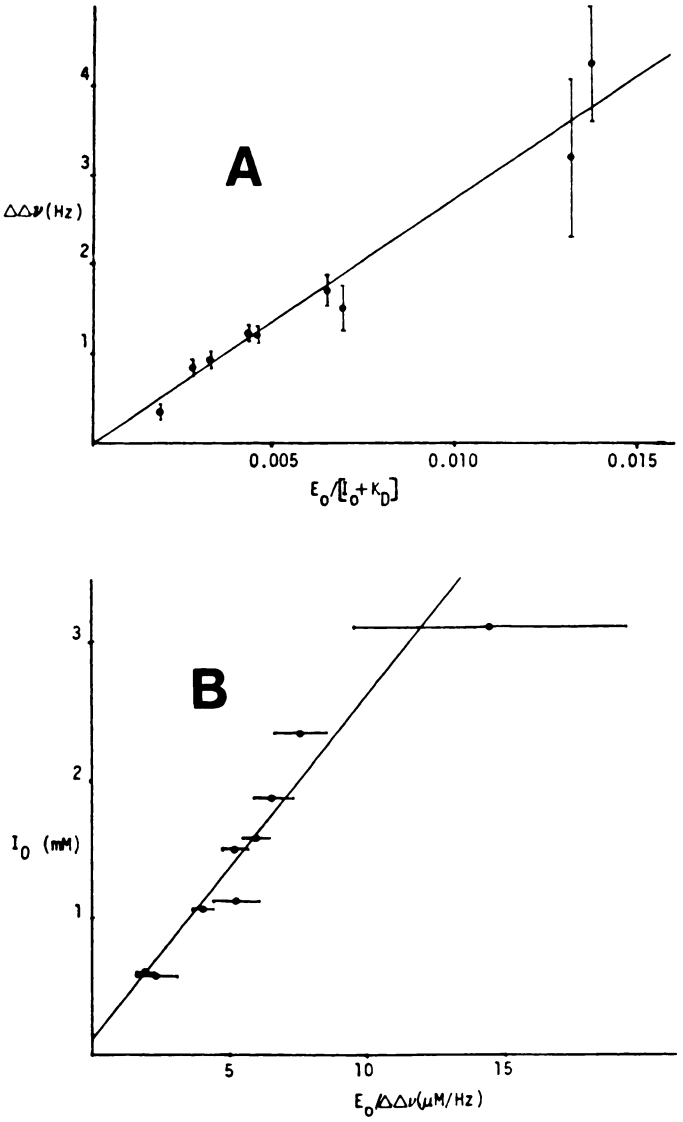


FIG. 3. *Extraction of bound line width, $\Delta\nu_B$, from net line broadening, $\Delta\Delta\nu$, as a function of eserine concentration, $I_0$, at fixed 11 S AchE 80,000 mol wt subunit concentration, $E_0$*

Plots A and B are based on Eqs. 7 and 8 (see text), for the *C*-methyl resonance at 100 MHz, 30°, pH 7.0. AchE is fully carbamylated under these conditions.

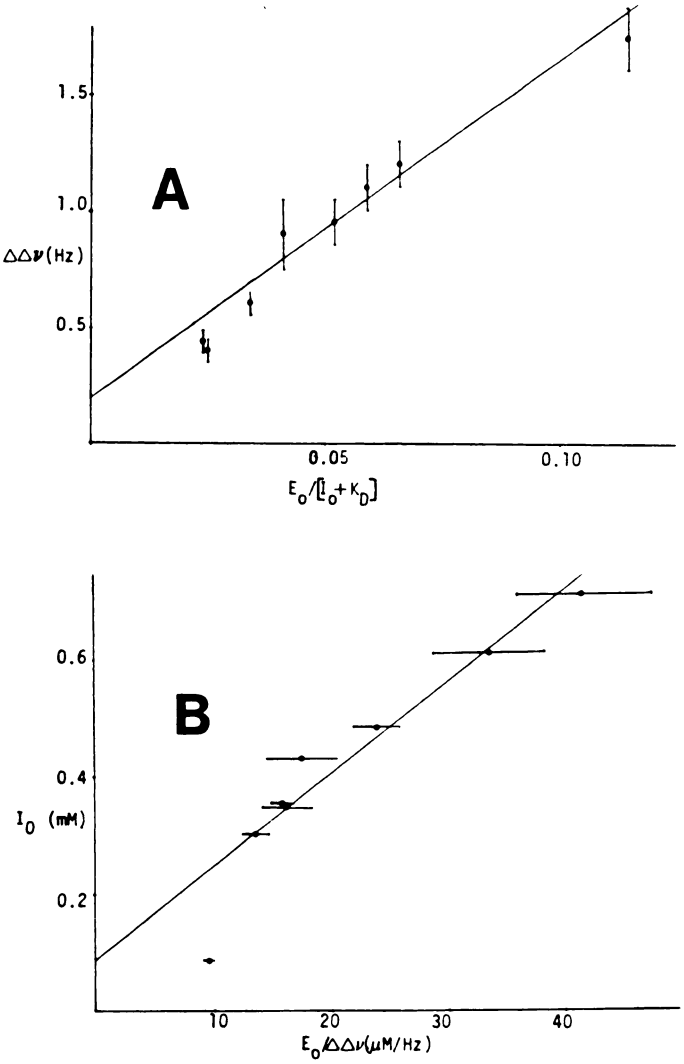


FIG. 4. *Extraction of bound methyl line width for interaction of phenyltrimethyl ammonium ion with 11 S AchE previously treated with methanesulfonyl fluoride*

Conditions are as in Fig. 3, except at 20° and 270 MHz.

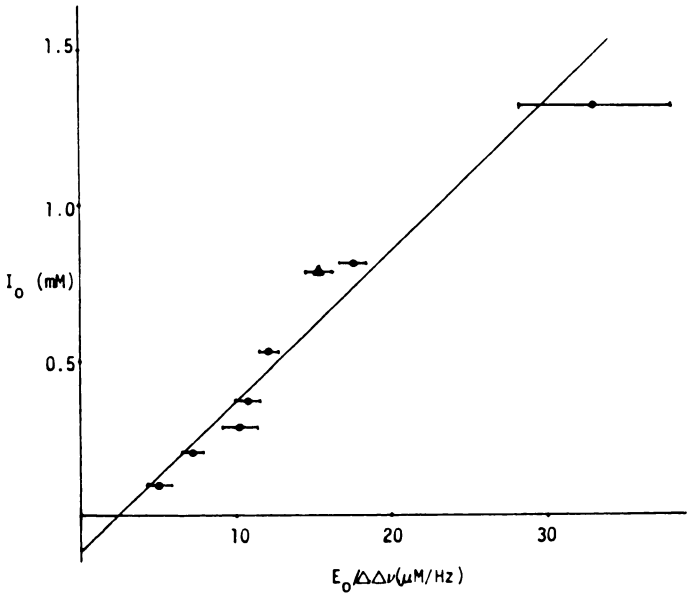


FIG. 5. *Extraction of bound methyl line width for interaction of atropine with methanesulfonyl AchE (11 S form) at 270 MHz, 20°*

The single data point (▲) was taken at 100 MHz, 20°.

aggregated at the concentrations used for NMR; however (see Materials and Methods), sucrose gradients prove that the present AchE remains in the 11 S form, with full activity, at these concentrations.

There are two remaining explanations for the observed zero line broadening. First, if exchange is very slow in the sense that $P_{BA} \ll (1/T_{2B})$, then for the maximal bound line width (see Theory) of about 500 Hz, and a typical fraction bound of $f_B = 0.02$, the observed line broadening (slow-exchange limit in Table 1) will be $\Delta(\Delta\nu) \ll 10$ Hz. Although this possibility cannot be ruled out, the relatively large $K_i$ values for Inhibitors *1–3* [$4.8 \times 10^{-3}$ M (27); $5.3 \times 10^{-5}$ M (27); and $4.0 \times 10^{-3}$ M (28)] render such a situation extremely unlikely. A second, much more probable, explanation is that the exchange is in the fast limit (bottom row in Table 1), with appreciable internal rotational motion at the binding site. For example, fast internal rotation about the N—C bond would reduce the bound line width by a factor of $[(3\cos^2\theta - 1)/2]^2 = 0.25$, since the H—H internuclear vector makes an angle, $\theta =$ 90°, with respect to the internal rotation N—C axis, reducing the bound line width to approximately 100 Hz if no other internal motions are present. Assuming a lower limit of 0.2 Hz as the minimal detectable experimental broadening, Eq. 4 (with $f_B = 0.02$) indicates that the minimal measurable bound line width is approximately 10 Hz. Thus, additional internal flexibility at this binding site must be present. An additional reduction in

TABLE 3

*Bound line width, $\Delta\nu_B$, for each of four inhibitors bound to 11 S AchE modified at the active-site serine residue*

| Inhibitor | AchE modification | $\Delta\nu_B$ | $K_D$ |
|---|---|---|---|
| | | *Hz* | *μM* |
| Eserine | Carbamylation | 273 ± 23[a]<br>248 ± 29[b] | 3.3 |
| Trimethylammonium chloride | Methanesulfonylation | 0[c] | |
| Phenyltrimethylammonium chloride | Methanesulfonylation | 14 ± 1<br>16 ± 2 | 53 |
| Atropine[d] | Methanesulfonylation | 97 ± 11 | |

[a] From a plot of

$$\frac{1}{T_2} - \frac{1}{T_{2_A}} \text{ versus } \frac{[E]_0}{K_D + [I]_0}:$$

see Eq. 7.

[b] From a plot of

$$[I]_0 \text{ versus } \frac{[E]_0}{\frac{1}{T_2} - \frac{1}{T_{2_A}}}:$$

See Eq. 8.

[c] $\Delta\Delta\nu = 0.2 \pm 0.1$ Hz, so that bound line width is too small to measure.

[d] From *C*-methyl peak.

observed bound line width of ≤30% may result from the nonspherical shape (19, 20) of 11 S AchE [frictional ratio = 1.3–1.4 (11)].

*Carbamylated enzyme.* Since we observe measurable line broadening of the *C*-methyl resonance of eserine on binding to carbamylated AchE, the fast-exchange limit must apply, based on the argument in the preceding paragraph and the measured $K_i = 7.6 \times 10^{-5}$ M (ref. 21) for eserine. The absence of any observed chemical shift in presence of enzyme indicates that the change in chemical shift on binding must be less than 50 Hz.

The bound *C*-methyl eserine line width determined from Fig. 3A or B is 273 ± 23 Hz or 248 ± 29 Hz, respectively, so that the two methods give essentially the same result. A self-consistency check is that the Fig. 3A weighted least-squares straight line through the data points passes through the origin, as required by Eq. 7. $K_D$ is too small to be determined from the intercept in Fig. 3B.

Since there is a measurable decarbamylation rate, one could imagine that the observed *C*-methyl broadening might represent a superposition of eserine and eseroline (the hydrolysis product) resonances; such a situation in fact occurs in observing acetylcholine methyl resonances in the presence of AchE (3–6). However, we synthesized eseroline and found that the *C*-methyl peak resonates at 1.46 ppm downfield from TSP, a full 5 Hz away from the *C*-methyl eserine peak.

Thus, the large bound *C*-methyl eserine line widths definitely indicate that eserine is firmly bound to the carbamylated AchE enzyme; this strongly suggests that the eserine binding site is spatially close to the active site serine residue.

*Sulfonylated enzyme.* The results with eserine suggested that chemical modification of the active-site serine residue (catalytic site) could affect ligand rotational mobility at the nearby anionic site. To test this hypothesis, the same inhibitors, *1–3*, were combined with methanesulfonyl AchE, and the results were monitored by proton NMR of the inhibitor methyl peaks.

Although no line broadening was observed for the smallest inhibitor, *1*, measurable line broadening for Inhibitors *2* and *3* provided data that could be reduced (Figs. 4 and 5) to give the bound line width data shown in Table 3. The justification for assuming the fast-exchange limit here is the same as in the preceding cases. As a further test, the atropine line width was observed at two different temperatures: the observed line width *decreased* by 0.2 Hz on increasing the temperature from 20 to 30°. [If the slow exchange limit were applicable, the line width should *increase* (because the exchange rate increases) on increase in temperature.] The same data confirm that the exchange rate is not in the intermediate exchange region (middle row of Table 1), because a change in field strength corresponding to NMR frequency of 100–270 MHz should increase the line broadening by a factor of about $2.7^2$, and the designated data point in Fig. 5 would be displaced significantly from the rest of the curve. Finally, it is possible that the $K_i$ values for binding to the sulfonylated enzyme are different (probably somewhat larger) than for binding to the unmodified 11 S enzyme, resulting in smaller values of $f_B$, with larger bound line widths and even more restriction of label flexibility at the bound site. The qualitative conclusions are thus essentially unaffected by the magnitude of $K_i$.

It is striking that the largest inhibitor, atropine (*3*) gives the largest bound line width (i.e., the most restricted rotational flexibility), whereas the smallest inhibitor (*1*) gives the smallest bound line width. Taken together, the above results strongly suggest the following: (a) the anionic binding site in unmodified 11.8 S AchE is probably a large pocket, within which inhibitors even as large as atropine can exhibit marked rotational flexibility when bound; (b) chemical modification at the active-site serine residue, either by carbamylation or sulfonylation, restricts the motion of the same inhibitors subsequently bound to the anionic site. Since the largest inhibitors are most restricted in motion by the active-site substituent, it seems highly likely that the anionic and catalytic sites are spatially proximal. In support of this view, very recent EPR studies of a series of spin-labeled alkylphosphonofluoridate inhibitors (in which the distance of nitroxide to serine was constant, but with increasing chain length of the alkyl group dangling above the serine) showed a restriction in motion of the nitroxide group on increase in alkyl chain length (29). The EPR results thus also point to a "roof" over the active site, leading to steric interference between different ligands bound in that cavity.

The obvious discrepancies (e.g., observed bound line width of less than 10 Hz for atropine with unmodified AchE, compared with the smallest value of 858 Hz found by Kato *et al.*) between the present results and previous literature values (7–10) merit comment. First, the experiments performed by Kato and co-workers were with squid AchE, rather than eel. However, recent reviews (e.g., ref. 30) suggest similar properties for AchE from different sources. The most likely difference is the low specific activity of the AchE used by Kato *et al.*, which was approximately 30% as active as the present preparation, if the acetylthiocholine assay applies equally to both species; binding of (for example) atropine to impurities in the preparation could have led to anomalously large broadening. Moreover, since the enzyme extract of Kato *et al.* contained no reported salt, it is likely that the AchE was aggregated; this could increase solution viscosity, and also increase the bound line widths for all binding sites (including impurities). Also, the AchE used by Kato *et al.* was prepared by freeze-drying, a process that markedly reduces the specific activity of eel AchE. Finally, the AchE used by Kato *et al.* was not homogeneous with respect to size and shape, whereas the present 11.8 S AchE is stable, nonaggregative, and globular.

## ACKNOWLEDGMENT

The authors wish to thank Dr. J. A. Benbasat for kinetic measurements of AchE inhibition.

## REFERENCES

1. Sykes, B. D., and M. D. Scott. Nuclear magnetic resonance studies of the dynamic aspects of molecular structure and interaction in biological systems. *Annu. Rev. Biophys. Bioeng.* 1:27–50 (1972).
2. Marshall, A. G., P. G. Schmidt, and B. D. Sykes. Effect of internal rotation on

nuclear magnetic relaxation times for macromolecules. *Biochemistry* **11:** 3875–3879 (1972).

3. Kato, G. Nuclear magnetic resonance study of the interaction between acetylcholine and horse serum cholinesterase. *Mol. Pharmacol.* **5:**148–155 (1969).
4. Kato, G. Acetylcholinesterase. II. A study by nuclear magnetic resonance of the acceleration of acetylcholinesterase by atropine and inhibition by eserine. *Mol. Pharmacol.* **8:**582–588 (1972).
5. Kato, G. Drug-biomolecule interactions: binding study of substrate and inhibitors to acetylcholinesterase using NMR. *J. Pharm. Sci.* **64:**488–493 (1975).
6. Krishnan, K. S., and P. Balaram. Nuclear magnetic resonance studies of the enzymatic hydrolysis of acetylcholine: a critical comment. *Mol. Pharmacol.* **13:**621–624 (1977).
7. Kato, G., J. Yung, and M. Ihnat. Nuclear magnetic resonance studies on acetylcholinesterase: the use of atropine and eserine to probe binding sites. *Mol. Pharmacol.* **6:**588–596 (1970).
8. Kato, G., J. Yung, and M. Ihnat. NMR studies of the interaction of eserine and atropine with acetylcholinesterase. *Biochem. Biophys. Res. Commun.* **40:**15–21 (1970).
9. Kato, G., and J. Yung. The use of nuclear magnetic resonance to describe the binding of atropine analogues to acetylcholinesterase. *Mol. Pharmacol.* **7:**33–39 (1971).
10. Kato, G. Acetylcholinesterase I. A study by nuclear magnetic resonance of the binding of inhibitors to the enzyme. *Mol. Pharmacol.* **8:**575–581 (1972).
11. Bon, S., M. Huet, M. Lemonnier, F. Rieger, and J. Massoulié. Molecular forms of *Electrophorus* acetylcholinesterase: molecular weight and composition. *Eur. J. Biochem.* **68:**523–530 (1976).
12. Anglister, L., and I. Silman. Molecular structure of elongated forms of electric eel acetylcholinesterase. *J. Mol. Biol.* **125:**293–311 (1978).
13. Rosenberry, T. L., and J. M. Richardson. Structure of 18S and 14S acetylcholinesterase: identification of collagen-like subunits that are linked by disulfide bonds to catalytic subunits. *Biochemistry* **16:**3550–3558 (1977).
14. Webb, G., and D. G. Clark. Acetylcholinesterase: differential affinity chromatographic purification of 11S and 18S plus 14S forms; the importance of multiple-site interactions and salt concentration. *Arch. Biochem. Biophys.* **191:**278–288 (1978).
15. Rosenberry, T. L., Y. T. Chen, and E. Bock. Structure of 11S acetylcholinesterase: subunit composition. *Biochemistry* **13:**3068–3079 (1974).
16. Morrod, P. J., A. G. Marshall, and D. G. Clark. Structural stability and composition of acetylcholinesterase purified by affinity chromatography from fresh electroplax tissue of *Electrophorus electricus*. *Biochem. Biophys. Res. Commun.* **63:**335–341 (1975).
17. McConnell, H. M. Reaction rates by nuclear magnetic resonance. *J. Chem. Phys.* **28:**430–431 (1958).
18. Swift, T. J., and R. E. Connick. NMR-relaxation mechanisms of $O^{17}$ in aqueous solutions of paramagnetic cations and the lifetime of water molecules in the first coordination sphere. *J. Chem. Phys.* **37:**307–320 (1962).
19. Werbelow, L. G., and A. G. Marshall. Internal rotation and methyl proton relaxation for macromolecules. *J. Am. Chem. Soc.* **95:**5132–5134 (1973).
20. Werbelow, L. G., and A. G. Marshall. Internal rotation and nonexponential methyl nuclear relaxation for macromolecules. *J. Magn. Reson.* **11:**299–313 (1973).
21. Marshall, A. G. *Biophysical Chemistry: Principles, Techniques, and Applications*. John Wiley & Sons, New York, pp. 199, 719, 1978.
22. Miller, D. B., J. P. Christopher, and D. Borrough. *Biophys. Chem.* **9:**9–14 (1978).
23. Bon, S., F. Rieger, and J. Massoulié. Proprietes des formes allongees de l'acetylcholinesterase en solution: rayon de stokes, densite et masse. *Eur. J. Biochem.* **35:**372–379 (1973).
24. Ellis, S. Studies on physostigmine and related substances. IV. Chemical studies on physostigmine breakdown products and related epinephrine derivatives. *J. Pharmacol.* **79:**364–372 (1943).
25. Marshall, A. G., T. Marcus, and J. Sallos. Solvent elimination from $^1$H NMR spectra: tunable notch filter. *J. Magn. Reson.* **35:**227–230 (1979).
26. Main, A. R., and F. L. Hastings. Carbamylation and binding constants for the inhibition of acetylcholinesterase by physostigmine (eserine). *Science (Wash. D. C.)* **154:**400–402, (1966).
27. Wilson, I. B., and J. Alexander. Acetylcholinesterase: reversible inhibitors, substrate inhibition. *J. Biol. Chem.* **237:**1323–1326 (1962).
28. Kato, G., E. Tan., and J. Yung. Acetylcholinesterase. Kinetic studies on the mechanism of atropine inhibition. *J. Biol. Chem.* **247:**3186–3189 (1972).
29. Pečar, S., M. Schara, M. Šentjurc, A. Štalc, and A. O. Župančič. The effect of aliphatic chain length of various spin label molecules bound to membrane acetylcholinesterase on the ESR spectra. *Stud. Biophys.* **77:**33–42 (1979).
30. Massoulié, J. The polymorphism of cholinesterases and its physiological significance. *Trends Biochem. Sci.* **5:**160–164 (1980).

**Send reprint requests to:** Dr. Alan G. Marshall, Departments of Chemistry and Biochemistry, Ohio State University, Columbus, Ohio 43210.